Early stages of formation of the Ag-Ni(111) interface studied by grazing incidence x-ray diffraction and x-ray photoelectron diffraction

C. Chambon,[1,3] A. Coati,[1] M. Sauvage-Simkin,[2,*] Y. Garreau,[1,3] J. Creuze,[4] A. Verdini,[5] A. Cossaro,[5] L. Floreano,[5] and A. Morgante[5,6]

[1]*Synchrotron SOLEIL, Saint Aubin BP 48, 91192 Gif-sur-Yvette Cedex, France*

[2]*Synchrotron SOLEIL and UR1-CNRS, Saint Aubin BP 48, 91192 Gif-sur-Yvette Cedex, France, associate to CNR-IOM, Laboratorio TASC, Trieste, Italy*

[3]*Université Paris Diderot, Sorbonne Paris Cité, MPQ, UMR 7162 CNRS, Bâtiment Condorcet, Case courrier 7021, 75205 Paris Cedex 13, France*

[4]*LEMHE-ICMMO, Bâtiment 410, Université Paris Sud, 15, Rue Georges Clémenceau, 91405 Orsay Cedex, France*

[5]*CNR-IOM, Laboratorio TASC, Basovizza, SS14, Km 163.5, 34012 Trieste, Italy*

[6]*Dipartimento di Fisica, Università di Trieste, via A. Valerio n.2, 34127 Trieste, Italy*

(Received 21 June 2011; revised manuscript received 27 September 2011; published 25 October 2011)

Ultra-thin Ag/Ni(111) reconstructed interfaces have been revisited by a combination of *in-situ* grazing incidence x-ray diffraction (GIXD) and x-ray photoelectron diffraction (XPD) in order to determine the growth mode and to evaluate the interface spacing. Evidence for predominance of single-layer growth in the early stages was obtained through the analysis of the x-ray diffraction rods from the Ag/Ni(111) $(\sqrt{52} \times \sqrt{52})$R13.9° reconstructed interface, whereas photoelectron diffraction patterns could reveal traces of second-layer Ag scatterers before full wetting of the substrate. Refinement of the atomic coordinates provided by quenched molecular dynamics simulation on the basis of the new x-ray data set enabled us to assess the Ag/Ni average interplanar distance, which was found unexpanded at 2.44 ± 0.07 Å, in contrast with recent determination by low-energy electron diffraction and microscopy. For increasing deposited amounts, both GIXD and XPD showed the expected features of two- and three-layer silver epitaxial overgrowths.

DOI: 10.1103/PhysRevB.84.165446 PACS number(s): 68.35.bd, 61.05.cp, 61.05.js

I. INTRODUCTION

Metal-on-metal epitaxy is a widely investigated topic, and among the various systems, the Ag-Ni couple has been the subject of many studies using a variety of experimental and theoretical approaches. Due to the large difference in atomic radii and cohesive energies, silver is almost non miscible[1] in the nickel bulk and shows a definite surface segregation trend. Accordingly, when depositing monolayer amounts of Ag on Ni(111), a sharp interface is observed, as demonstrated by the occurrence of quantum well states in the electronic structure,[2] and a quasi relaxed Ag thin film is formed. However, due to a non negligible interaction with the Ni substrate, the Ag layer retains an epitaxial relationship revealed by low-energy electron diffraction (LEED) and moiré patterns on scanning tunneling microscopy (STM) images.[3–7] Several commensurate superstructures have been identified from a collinear 7 × 7 to different non collinear phases rotated by a few degrees, the supercell area being always close to that of the 7 × 7 case.[8,9] Quenched molecular dynamics (QMD) simulations[10] have compared the relative energies of these various epitaxial interfaces and clearly established the higher stability of the non collinear ones, in particular the $(\sqrt{52} \times \sqrt{52})$R13.9°. Detailed studies of the early stages of growth have raised a controversy on the actual wetting of the Ni surface by silver: in a previous work, it was deduced on the basis of STM measurements and Auger data calibration of the deposited amount that silver grew initially in the form of two-layer films,[11,12] whereas other groups were in favor of single-layer growth.[3,5–7] Scanning tunneling microscopy measurements provide information on the substrate partial coverage by silver and on the apparent height of the steps present on the surface between silver-covered and bare regions. In all studies, the STM-measured heights were comprised between 2.7 and 3 Å, values much larger than any interplanar distance in silver or in nickel. They were interpreted as the signature of a two-layer overgrowth by one group and a single-layer overgrowth by the other ones, since it was unclear whether this measured step height was a real morphological feature or the result of electronic effects due to different density of states and work function between clean and Ag covered surfaces. In a recent quantitative intensity-voltage [I(V)]-LEED and low-energy electron microscopy (LEEM) study,[13] the initial stages of growth of this interface were revisited in great details as a function of growth temperature and coverage: the occurrence of the various reconstructed interfaces was confirmed, and in addition, the successive interlayer spacings were assessed on the basis of a simplified model, which yielded a truly expanded Ag/Ni interface distance of 2.8 ± 0.1 Å. This last result is in contradiction with the value obtained by QMD[10] and, as will be shown later, is not confirmed by our grazing incidence x-ray diffraction (GIXD) results. Indeed, in order to gather complementary information on this interface, a combined study had been launched independently, coupling soft x-ray photoelectron diffraction (XPD) on the Ag emission, a technique sensitive to the presence or absence of out-of-plane neighbors, and GIXD, sensitive to the actual stacking of Ag and Ni in the ordered superstructures. A crucial issue was the determination of the actual substrate surface coverage corresponding to a calibrated deposited amount of silver. In this paper, this issue was addressed by calibrating the evaporation rate with a quartz oscillator and evaluating the

fraction of uncovered Ni surface by dosing the sample with CO and monitoring the adsorption by C 1*s* and O 1*s* core-level soft x-ray photoelectron spectroscopy (XPS).[14]

This series of experiments coupling in-situ electron spectroscopy in the soft X-ray regime and X-ray diffraction in a harder energy range has been performed on the ALOISA beamline of the ELETTRA synchrotron (Trieste-Italy). This experimental station is unique to offer such coupling opportunities.[15]

II. EXPERIMENTAL

The sample was an Ni single crystal (diameter 9 mm, height 2 mm) with a (111) polished surface. It was introduced in the ALOISA UHV preparation chamber and cleaned by several cycles of sputtering by 1.5-kV argon ions and annealing at about 900 K. The absence of contaminants was checked by XPS with a photon energy of 675 eV. Silver deposition was done at room temperature with an e-beam evaporator (Omicron-EFM3) calibrated with a quartz microbalance. The uncovered Ni fraction was estimated by measurement of the C 1*s* and O 1*s* photoemission after CO dosing. When exposed to 20 L of CO, a nickel substrate is fully covered by the gas, whereas no CO sticking occurs on Ag islands.[14] Taking as a reference the XPS from the bare Ni surface, the C and O photoemission intensity is directly proportional to the Ni area uncovered by Ag islands.

Two series of experiments were conducted, the first one with an evaporation rate of 0.073 ± 0.008 equivalent ML/min, where four deposits corresponding to 0.58, 0.87, 1.5, and 2.9 equivalent ML with 10% accuracy have been performed, and the second one with the rate of 0.039 ± 0.004 equivalent ML/min, where six samples have been prepared corresponding to 0.39, 0.78, 1.2, 1.6, 3.1, and 6.2 equivalent ML with 10% accuracy (1 ML is defined as a relaxed close packed 111 silver layer). Before each new deposit, the sample was sputtered and annealed.

In the first series of Ag growth, the Ni surface was found to be fully covered by Ag (no CO sticking) from the coverage of 1.5 ML on. In the second series, CO sticking was found until 1.6 ML.

X-ray photoelectron diffraction angular patterns from the Ni 3*p* and Ag 3*d*5/2 core levels were collected at a photon energy of 600 and 900 eV, respectively, for a few representative films of both series. Grazing incidence x-ray diffraction data were collected at a photon energy of 7 keV for the 0.58 and 1.5 ML films of the first series. Photoelectron diffraction and x-ray diffraction data presented in the following were recorded after annealing the samples at 400 °C.

III. RESULTS AND DISCUSSION

A. Addressing the initial Ag deposit thickness through CO dosing

The actual thickness of the Ag islands in the initial state can be estimated by comparing the Ag covered fraction derived from CO dosing with the Ag deposited amount derived from the quartz oscillator data. The results obtained in the two series of experiments, prior to full Ag coverage, are displayed in Fig. 1. The 0.58- and 0.87-ML deposits performed in

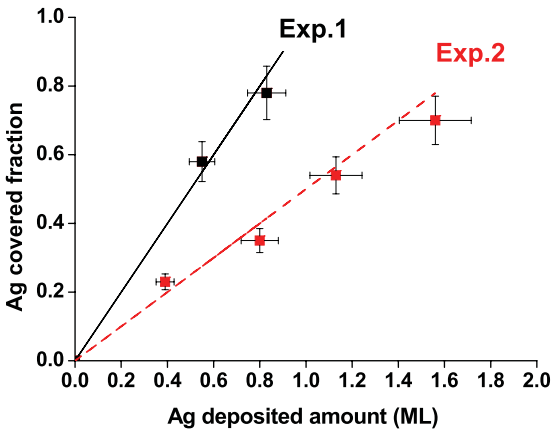

FIG. 1. (Color online) Ag covered fraction as a function of the Ag deposited amount for the two series of experiments. Straight lines correspond, respectively, to monolayer growth (black full line) and bilayer growth (red dashed line). The error bars correspond to an accuracy of 10% for both measurements methods.

experiment 1 (black square labels), where the Ag covered fraction is found equal to the deposited amount, can be interpreted as monolayer silver islands, which is in agreement with the published literature[3,5] but contradicts our previous STM findings.[11] It will be shown that GIXD data collected on this series of samples are also in favor of monolayer deposits in the early stages.

The results obtained by the same CO dosing technique in the second series of samples prepared in experiment 2 (red filled squares in Fig. 1) are, on the contrary, representative of bilayer growth since the covered fraction is about half the nominal deposited amount. It is worth mentioning here that XPD data collected on all samples from this second series revealed a more disordered interface which may be due to very small initial nuclei induced by surface defects or impurities. In the following, we will restrict ourselves to the XPD and GIXD data collected on the series of samples prepared in experiment 1. The first conclusion of this approach is that the initial growth mode of Ag on Ni(111) may indeed correspond to monolayer or bilayer depending critically on the state of the substrate surface. One cannot also exclude an effect of the

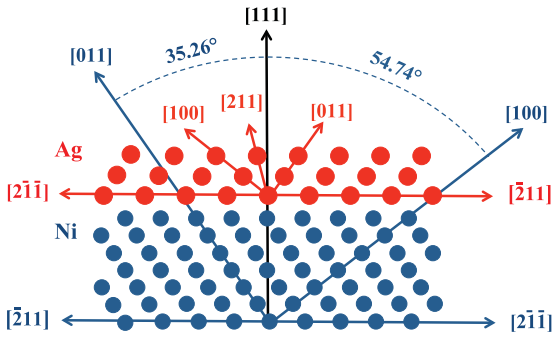

FIG. 2. (Color online) Main forward scattering directions for a three-layer Ag deposit (large red dots) on Ni(111) (small blue dots) in a twinned fcc stacking relationship, viewed in the (0 1 −1) plane. Red arrows and labels refer to the Ag lattice.

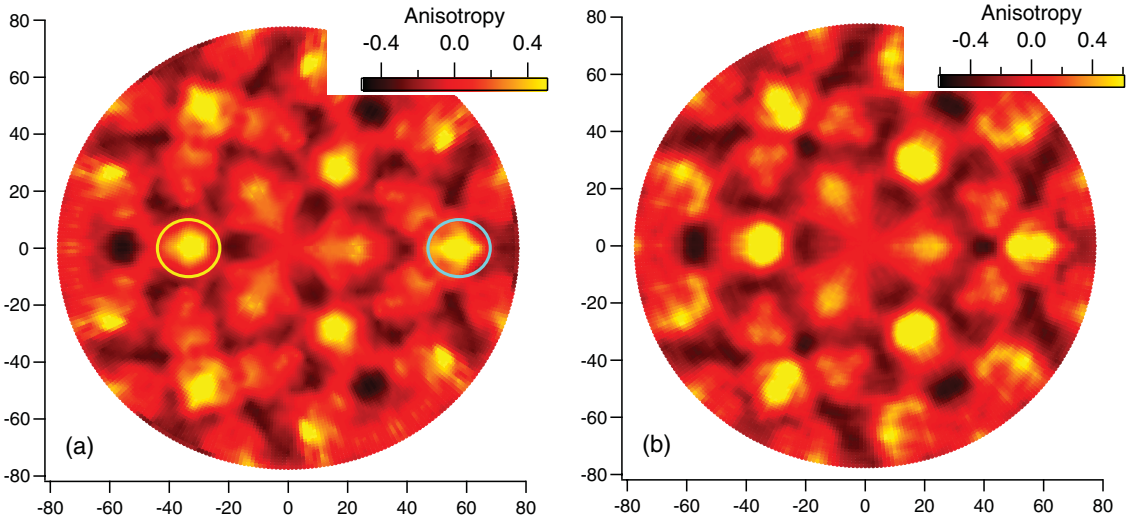

FIG. 3. (Color online) (a) Experimental and (b) simulated XPD patterns of the clean Ni substrate (Ni 3p core-level electrons).

lower evaporation rate used in experiment 2, which could favor bilayer growth.

B. Soft x-ray photoelectron diffraction

X-ray photoelectron diffraction data were recorded on the Ni 3p core levels (binding energy 3p3/2: 66eV; 3p1/2: 68 eV) and Ag 3d5/2 core level (binding energy 368 eV). In both cases, the incident photon energy was adjusted to bring the electron kinetic energy to the same value of about 530 eV, a regime where forward scattering is dominant. However, backscattering and multiple scattering might also be present and were taken into account in the simulations. Full angular patterns and angle scans (polar or azimuthal) were recorded on the clean nickel and after several Ag deposits. For (111)-oriented fcc materials, the most significant information on the out-of-plane structure is contained in {01-1} planes (Fig. 2).

As shown in Fig. 2, the occurrence of a second Ag layer will manifest through the appearance of strong maxima in the forward scattering of Ag core-level electrons along $[100]_{Ag}$ and $[011]_{Ag}$ directions (red labels in Fig. 2) in $\langle -211 \rangle$ azimuth separated by 180° (60°) according to the overall threefold symmetry of the crystal. The signature of the third Ag layer will be a peak in the $[211]_{Ag}$ direction in the same azimuth as the $[100]_{Ag}$. First, the case of rather thick layers will be considered: the full patterns collected for the clean Ni substrate and for the silver 2.9-ML sample are presented in Figs. 3 and 4 together with best fit simulations obtained with the MSCD package.[16]

The peaks corresponding to first out-of-plane neighbors in high-symmetry azimuths are outlined by yellow and light blue circles. It thus appears from direct inspection that the Ni and Ag lattices are almost related by a 180° rotation, which

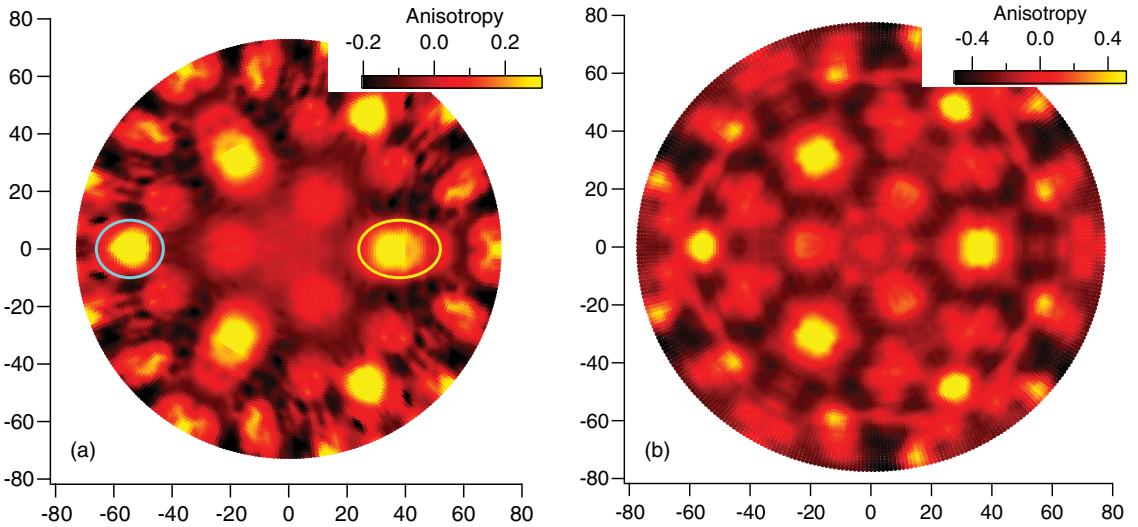

FIG. 4. (Color online) (a) Experimental XPD patterns of the 2.9-ML Ag deposit; (b) simulated pattern for 3-ML Ag (Ag 3d5/2 core-level electrons).

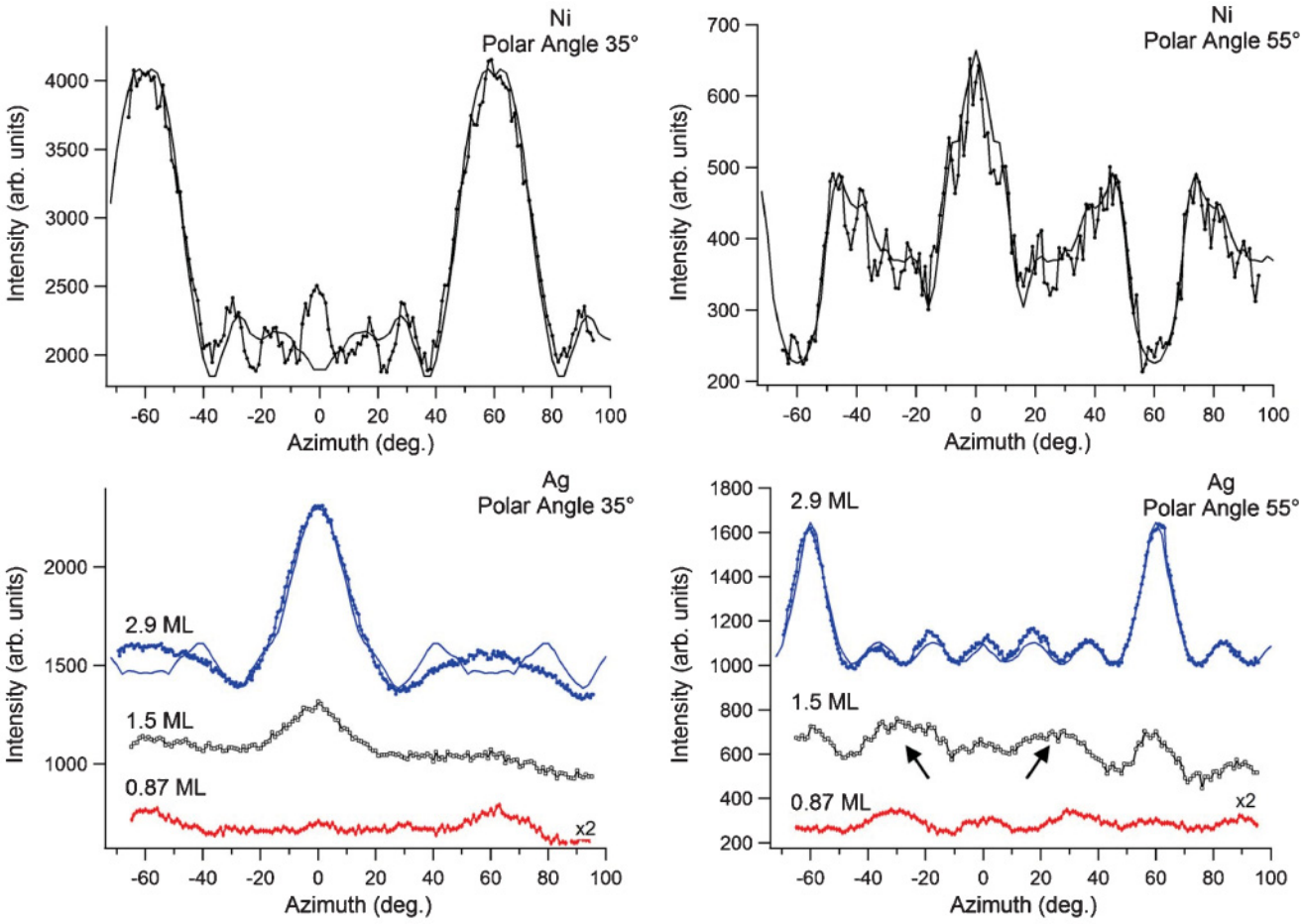

FIG. 5. (Color) Azimuthal scans at two polar angles for bulk Ni (top panels) and three Ag epilayers (bottom panels). Twin relationship between the 2.9-ML Ag deposit and the substrate is evident. Simulations are displayed by smooth thin lines. The arrows point to features unaccounted for by epilayer scattering. Ag curves are shifted for the sake of clarity.

means a reverse fcc stacking for the silver overlayer as the one schematically presented in Fig. 2:

$$\mathrm{AgA'C'B'}\ldots/\mathrm{Ni}:\mathrm{ABC}\ldots$$

A predominance of a reverse orientation in the Ag/Ni(111) growth has already been reported by Ito *et al.*[17] for deposition temperatures above 300 K with a totally reverse growth above 450 K. In the present case, deposition was performed after sputtering and annealing of the substrate at 900 K and cooling down. However, the actual deposition temperature might have been still above room temperature, which favors a reverse growth, according to Ref. 17. It should be mentioned that, for the Au/Ni(111) couple, an oscillatory behavior between normal and reverse orientation as a function of deposition temperature has been observed by Umezawa *et al.*[18] The controlling parameters of the growth orientation are thus not fully understood yet.

A closer inspection of the raw data (not presented here) has revealed a small rotation of about 1–2° between the in-plane crystallographic directions of both lattices, in agreement with the non collinear commensurate supercells identified in previous works.[10] Fast azimuthal scans, with a reduced energy range on photoemission peaks were collected at the two polar angles characteristic of out-of plane first nearest neighbors (Fig. 5). The twin relationship between the nickel substrate and the 2.9-ML-thick silver deposit is evidenced, both series of scans comparing very well with simulations (shown as thin lines), and the slight discrepancies might be due to defects such as stacking faults or to the minor presence of the other twin individual. For the two thinner deposits, the relationship is primarily a reverse stacking for the 1.5-ML sample, as shown clearly in the midcurve of the bottom left panel and more likely a direct stacking for the 0.87-ML sample. However, in both cases, a satisfactory fit could not be reliably obtained. In particular, the modulations pointed by the arrows in the lower right panel could not be reproduced by any combination of Ag layers. These features could be tentatively attributed to Ag atoms embedded on substitutional sites in the second layer of the Ni substrate. Although such a surface alloy is considered unstable and has not been observed by other authors,[13,19] the annealing at 400 °C may have induced a limited Ag interdiffusion within the substrate, as was reported by Li *et al.* in an Ag/Ni multilayer sample.[20]

For the thinnest deposit (0.58 ML), the experimental XPD pattern is presented in Fig. 6(a), while the simulation performed with a reconstructed Ag single layer having the $(\sqrt{52}\times\sqrt{52})\mathrm{R}13.9^\circ$ symmetry is displayed in Fig. 6(b). A fairly good matching is obtained at large polar angles (dots

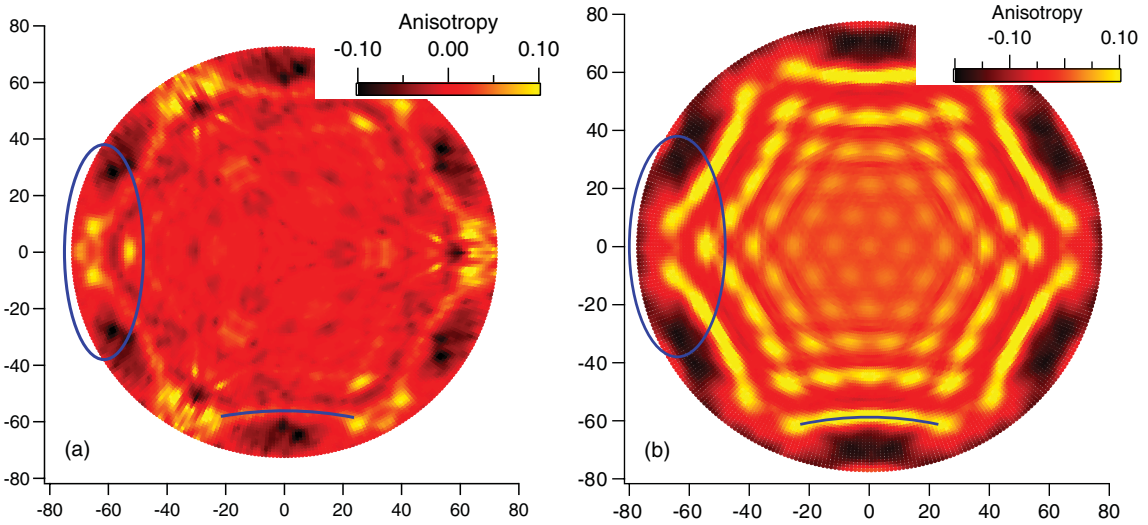

FIG. 6. (Color online) (a) Experimental XPD pattern for a 0.58-ML silver deposit on Ni(111) (Ag $3d5/2$). (b) Simulated XPD pattern from a 1-ML silver, $(\sqrt{52} \times \sqrt{52})$R13.9° reconstructed on Ni(111). Well-fitted areas are outlined, and a threefold symmetry is visible in the experimental pattern.

and arcs outlined in the figure). Nevertheless, the experimental pattern shows a weak threefold symmetry, which is not reproduced in the simulation. A possible reason could be the emission from substituted silver atoms invoked before and embedded in a bulk threefold environment or from traces of thicker Ag islands.

The conclusion of this series of measurements is that if monolayer growth is indeed the dominant mode in the early stages of formation of the Ag/Ni(111) interface, XPD is able to demonstrate that bilayer islands do exist in minor proportion before full wetting, possibly together with isolated silver atoms embedded in the Ni lattice. It should be remarked here that the hypothesis of Ag atoms forming a lattice gas on the substrate surface proposed in Ref. 13 did not lead to backscattering XPD features compatible with the present results at least for simple adsorption sites (threefold hollow or on top sites).

C. Grazing incidence x-ray diffraction data

Grazing incidence x-ray diffraction, whose interpretation relies on the simple x-ray kinematical theory, is the most appropriate tool to obtain the atomic positions in ordered surface structures. As recalled above, the Ag/Ni(111) interface presents several ordered phases characterized by large supercells and indeed the reflexion high-energy electron diffraction (RHEED) patterns observed in the present experiments, just after depositions, showed reconstructions close to 7×7.

In-plane GIXD maps and rod data were collected at 7 keV on the 0.58- and 1.5-ML samples. In both cases, the surface diffraction peaks were split due to the presence of several commensurate superstructures with slightly different rotation angles of the order of 1° or 2° with respect to the Ni substrate. Rods were measured only on the two more intense in-plane peaks of the superstructures, which would be crystal truncation rods (CTR) in an Ag(111) basis and are for the sake of

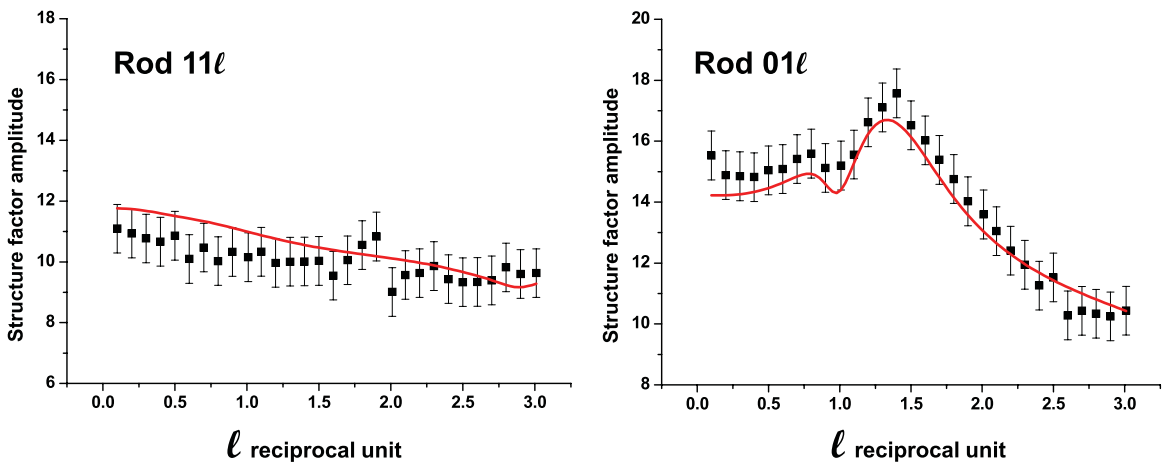

FIG. 7. (Color online) Comparison between experimental (0.58-ML sample: square dots) and fitted (continuous curve) structure factor amplitudes for the 1-ML Ag/Ni(111), $(\sqrt{52} \times \sqrt{52})$R13.9° reconstructed surface.

TABLE I. Input average values from QMD simulations (Ref. 10) and measured average interface distances from published LEED analysis (Ref. 13) and from the present GIXD experiment.

FWHM Ag QMD[10]	FWHM Ni_t QMD	$\langle d_{int}\rangle$ QMD	$\langle d_{int}\rangle$ LEED[13]	$\langle d_{int}\rangle$ GIXD
0.11 Å	0.25 Å	2.26 Å	2.8 ± 0.1 Å	2.44 ± 0.07 Å

simplicity referred to as the 01ℓ and 11ℓ rods. The data were fitted with the ROD software[21] using as input file the atomic coordinates derived by QMD minimization of the interface energy.[10] Since such large surface cells involve more than 50 atoms per layer, the refinement was not performed on individual atoms but only concerned the Ag-Ni average interface spacing $\langle d_{int}\rangle$ and a scale factor. In addition, an out-of-plane Debye–Waller parameter was fixed at two for the top Ag layer(s). The comparison between experimental data collected on the 0.58-ML sample and simulations obtained by fitting the interface spacing in the supercell of the $(\sqrt{52} \times \sqrt{52})$R13.9° commensurate structure for 1-ML Ag/Ni(111) is displayed in Fig. 7.

The fit was driven by the reliability factor defined as:

$$R = \frac{\sum \left| F_{hkl}^{obs} - \left| F_{hkl}^{calc} \right| \right|}{\sum F_{hkl}^{obs}}$$

where F_{hkl}^{obs} and $|F_{hkl}^{calc}|$are respectively the square roots of the corrected measured intensities and the moduli of the calculated structure factors. The best fit value was $R = 0.045$. The error bars on data points include statistical errors and additional systematic errors induced by the scaling of different rods. Both the Ag layer and the Ni top layer, labeled Ni_t, are found highly corrugated from the QMD simulations, as shown in Table I, where the QMD derived full width at half maximum (FWHM) of each layer roughness is indicated.

The average interface distance $\langle d_{int}\rangle$ is then given by:

$$\langle d_{int}\rangle = c.\langle \Delta z\rangle$$

where $c = 6.0992$ Å is the length of the [111] lattice vector in fcc Ni and $\langle \Delta z\rangle$ is defined by:

$$\langle \Delta z\rangle = \langle z_{Ag}\rangle - \langle z_{Ni_t}\rangle.$$

Table I shows that the mean interface distance derived from QMD is constricted to 2.26 Å, a value intermediate between Ag and Ni bulk (111) spacing. Since the value obtained from recent [I(V)]-LEED data[13] is, on the contrary, an expanded spacing of 2.8 Å, the GIXD rod data have been fitted with two input coordinates: the first ones used the QMD set, and the second used an expanded set where the mean interface distance was placed at 2.8 Å. Both fitting processes converge to the same value of 2.44 ± 0.07 Å for the average interface distance as reported in Table I. This value is close to the fcc silver (111) interplanar spacing (2.35 Å), and the larger value measured at steps by STM is thus to be attributed to electronic effects only. The discrepancy with the LEED result could be due to the simplified fully strained model introduced in the dynamic LEED calculations.[13] However, it should be remarked that the actual local distance between Ag and Ni levels varies from 2.64 Å for on top positions to 2.36 Å for quasi threefold hollow sites in the presently refined reconstructed $(\sqrt{52} \times \sqrt{52})$R13.9° surface.

The same two rods were measured on the 1.5-ML sample. This deposited amount implies that the Ag epilayer is a mixture of single and bilayer areas since no bare nickel areas were detected by CO dosing. Indeed, the rods could not be fitted by a homogeneous bilayer model. The fit was thus performed varying the ratio of mono- and bilayer areas where the coordinates used for monolayer areas were kept fixed at those obtained in the previous thin sample, and the bilayer ones were coming from the QMD calculation of a two-layer $(\sqrt{52} \times \sqrt{52})$R13.9° reconstructed interface.[10] The attempt to fit the interlayer spacings Ag-Ag and Ag-Ni_t in the bilayer case did not bring a significant improvement, possibly in view of the limited data set. The final result is displayed in Fig. 8, where the optimal ratio is 75% single layer and 25% bilayer (reliability factor $R = 0.075$), leading to a total amount of silver in the ordered deposit of 1.25 ML The missing silver amount could be present in small patches not contributing to the long-range order signal sorted out in the x-ray diffraction data or even to embedded isolated atoms as assumed in the XPD section.

As mentioned above, several rotated phases were present, and for the sake of consistency, the GIXD data were also fitted with the coordinates derived from QMD

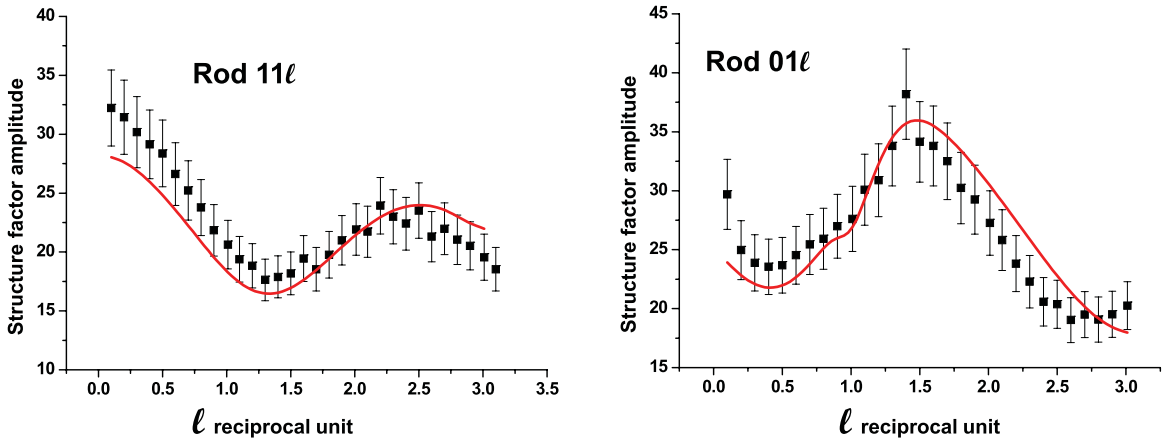

FIG. 8. (Color online) Comparison between experimental data (square dots) and fit (continuous line) for the 1.5-ML sample.

simulations of a $(\sqrt{57} \times \sqrt{57})$R6.59° reconstructed interface: the results in terms of average interface spacing and ratios of the two thicknesses in the thicker sample were found similar.

IV. CONCLUSION

This combined study by GIXD and XPD has demonstrated that the majority of long-range ordered areas in the submonolayer deposition regime is indeed one monolayer thick with an average interface distance of 2.44 Å, much lower than the apparent step height obtained in STM determination. However, before full wetting, the presence of two-layer small islands could be detected with XPD, which requires only short-range orientational order. X-ray photoelectron diffraction left open the possibility of embedded Ag atoms in the upper layers of the substrate. In addition, the independent determination of the uncovered substrate fraction by CO dosing as a function of the deposited amount has provided a crosscheck of the island height determination and shown that defects at the substrate surface might induce a different growth behavior.

The richness of a multitechnique approach is clearly evidenced for this study of a complex system and outlines the importance of the specific sensitivity of each method.

ACKNOWLEDGMENTS

MSS wishes to thank A. Tejeda (Institut Jean Lamour-Nancy and SOLEIL) for fruitful discussions. A. Coati acknowledges the support of the European Community seventh framework program (FP7/2007-2013) under Grant Agreement No. 226716.

*michele.sauvage@synchrotron-soleil.fr

[1] X. J. Liu, F. Gao, C. P. Wang, and K. Ishida, J. Electron. Mater. **37**, 210 (2008).
[2] A. Varykhalov, A. M. Shikin, W. Gudat, P. Moras, C. Grazioli, C. Carbone, and O. Rader, Phys. Rev. Lett. **95**, 247601 (2005).
[3] R. T. Vang, K. Honkala, S. Dahl, E. K. Vestergaard, J. Schnadt, E. Laegsgaard, B. S. Clausen, J. K. Norskov, and F. Besenbacher, Surf. Sci. **600**, 66 (2006).
[4] F. Besenbacher, L. P. Nielsen, and P. T. Sprunger, in *The Chemical Physics of Solid Surfaces*, edited by D.A. King and D. P. Woodruff, Vol. 8 (Elsevier, New York, 1997), Chap. 6, p. 207.
[5] S. Nakanishi, K. Umezawa, M. Yoshimura, and K. Ueda, Phys. Rev. B **62**, 13136 (2000).
[6] K. Aït-Mansour and O. Gröning, Surf. Sci. **604**, 872 (2010).
[7] V. M. Trontl, P. Pervan, and M. Milun, Surf. Sci. **603**, 125 (2009).
[8] L. G. feinstein, E. Blanc, and D. Dufayardn, Surf. Sci. **19**, 269 (1970).
[9] S. Mroz and Z. jankowski, Surf. Sci. **454-456**, 702 (2000).
[10] C. Chambon, J. Creuze, A. Coati, M. Sauvage-Simkin, and Y. Garreau, Phys. Rev. B **79**, 125412 (2009).
[11] C. Chambon, A. Coati, and Y. Garreau, Surf. Sci. **602**, 2363 (2008).
[12] C. Chambon, A. Coati, and Y. Garreau, Surf. Sci. **604**, 875 (2010).
[13] A. Meyer, J. I. Flege, R. E. Rettew, S. D. Senanayake, T. Schmidt, F. M. Alamgir, and J. Falta, Phys. Rev. B **82**, 085424 (2010).
[14] A. P. Shapiro, T. Miller, and T. C. Chiang, Phys. Rev. B **37**, 3996 (1988).
[15] G. A. Rizzi, A. Cossaro, M. Petukhov, F. Sedona, G. Granozzi, F. Bruno, D. Cvetko, A. Morgante, and L. Floreano, Phys. Rev. B **70**, 045412 (2004).
[16] MSCD code is freely distributed by Y. Chen and M. A. Van Hove, at [http://electron.lbl.gov/mscdpack/mscdpack.html]; see also Y. Chen, F. J. Garcia de Abajo, A. Chasse, R. X. Ynzuna, A. P. Kaduwela, M. A. VanHove, and C. S. Fadley, Phys. Rev. B **58**, 13121 (1998).
[17] T. Ito, K. Umezawa, and S. Nananishi, Appl. Surf. Sci. **130-132**, 497 (1998).
[18] K. Umezawa, S. Nakanishi, and W. M. Gibson, Phys. Rev. B **57**, 8842 (1998).
[19] B. Aufray, H. Giordano, B. Legrand, and G. Treglia, Surf. Sci. **307-309**, 531 (1994).
[20] Z. C. Li, D. P. Yu, and B. X. Liu, Phys. Rev. B **65**, 245403 (2002).
[21] E. Vlieg, J. Appl. Cryst. **33**, 401 (2000).